

Magnetoresistance in ferromagnetically contacted single-wall carbon nanotubes

Ane Jensen,* Jonas R. Hauptmann, Jesper Nygård, and Poul Erik Lindelof

Nano-Science Center, Niels Bohr Institute, University of Copenhagen, Universitetsparken 5, DK-2100 Copenhagen, Denmark

(Received 22 December 2004; published 7 July 2005)

We present two-terminal magnetotransport measurements on single-wall carbon nanotube devices, where one or two of the terminals are ferromagnetic. Both ferromagnetic semiconductor [(Ga,Mn)As] and metal (Fe) contact materials have been investigated. In both types of devices we have observed strong hysteretic magnetoresistance below 30 K. The magnetoresistance features develop into large peaks and dips at subkelvin temperatures and they are present even with only one ferromagnetic terminal.

DOI: [10.1103/PhysRevB.72.035419](https://doi.org/10.1103/PhysRevB.72.035419)

PACS number(s): 72.25.Hg, 73.63.Fg

The possibility of controlling electron transport by means of the spin degree of freedom, in short spintronics, has drawn recent attention, as spintronic devices may have potential for applications in future commercial electronics, and generate insight into fundamental properties of the electron spin physics in solids.¹ Spin-polarized transport in mesoscopic and low dimensional systems has gained particular interest.²⁻⁵ Within the line of this work we explore spin-polarized transport in single-wall carbon nanotubes (SWNTs), which already possess unique electronic properties.^{6,7} These nanotubes may form a perfect spin-transport medium as their electron transport is one dimensional and ballistic with expected long spin relaxation length as well as negligible spin orbit effects.

Spin-polarized transport may be investigated in carbon nanotubes contacted by two ferromagnetic terminals.⁴ Investigations of SWNT quantum dots display that the effective size of the nanotube island is roughly equal to the separation between the terminals;⁸ thus the electrical contact between nanotube and terminal must be formed at the very edge of the terminal, with an area which may be comparable to the diameter of the tube. Hereby, the nanotube is supposed to probe a single ferromagnetic domain, since the domains, presumably of micrometer size, are much larger than the area of the tube/terminal contact. Sweeping an external magnetic field will cause abrupt alternation between different magnetization configurations of the contacting areas. In the simplest picture the magnetizations of the contacting domains are saturated in parallel and antiparallel configurations, as illustrated by the sequence in Figs. 1(a)–1(c). Accordingly, a difference in resistance, a magnetoresistance, from a spin-valve effect may be expected. This change in resistance has previously been estimated from the model first described by Julliere⁹ in the context of spin-polarized transport between two ferromagnetic metals separated by a tunnel barrier. However, in nanotube devices the nanotubes form conducting channels between the magnetic electrodes and the model is not directly applicable to these systems. Observation of magnetoresistance has been ascribed to a spin-valve effect in ferromagnetically contacted multiwall^{4,10-13} and SWNTs.^{14,15} A strong diversity in magnitude and changes between positive and negative magnetoresistance have, however, been observed.

We have fabricated two types of nanotube devices with ferromagnetic source and drain terminals, namely, ferromag-

netic metallic iron and an epitaxially grown ferromagnetic semiconductor (FS) (Ga,Mn)As (see Fig. 1). We denote the two types Fe-NT-Fe and FS-NT-FS, respectively. The Fe-NT-Fe devices were prepared from chemical vapor deposition grown tubes¹⁶ on a n^+ Si substrate used as a back gate capped by 300 nm insulating SiO₂ with terminals of 50 nm Fe capped *in situ* by 15 nm Au.¹⁵ Additionally, we have investigated one type of reference device with a source of nonmagnetic metals, Cr/Au of 5 nm/30 nm, and a drain of (Ga,Mn)As, denoted by M-NT-FS, Fig. 1(d). The FS-NT-FS and M-NT-FS devices are grown by molecular beam epitaxy (MBE) on a highly doped GaAs substrate, where laser ablated SWNTs from the group of Smalley (Rice University) are introduced during a growth interrupt. Electron beam lithography and wet etch are used to define the terminals of (Ga,Mn)As. The tubes are separated from the back gate of highly doped GaAs by a 400 nm electrical superlattice barrier of GaAs/AlAs. Details for the device fabrication of the epitaxially grown (Ga,Mn)As terminals have been published elsewhere.¹⁷

Measurements are performed in the temperature range from 300 mK to room temperature with a dc setup as sketched in Fig. 1(a). The external magnetic field B is applied in the plane of the ferromagnetic terminals. The conductance G is defined as I/V in the linear regime. The two-terminal resistance ($1/G$), which is in the megaohm range for most of these devices, is dominated by the contact barrier at the terminal/nanotube interfaces. For a SWNT device the one-dimensional quantized resistance contributes $h/(4e^2) \approx 6.5$ k Ω . Moreover, the low temperature transport characteristics indicate that the nanotube transport is mostly ballistic and thus the intrinsic nanotube resistance is negligible. The series resistance of the ferromagnetic terminals can also be neglected. Metallic behavior of the SWNTs is detected in all devices reported here.

Results from two devices with Fe terminals are presented in Fig. 2. We find periodic oscillations in G vs gate voltage V_g at low temperatures [Fig. 2(a)]. This is due to Coulomb blockade,^{8,18,19} which is typical for nanotubes with tunnel contacts, making the device behave as a quantum dot. Periodic Coulomb blockade oscillations indicate that the tube behaves as a single quantum dot. We report solely on devices which display clear Coulomb blockade oscillations, to ensure our results come from ballistic transport in regular nanotube

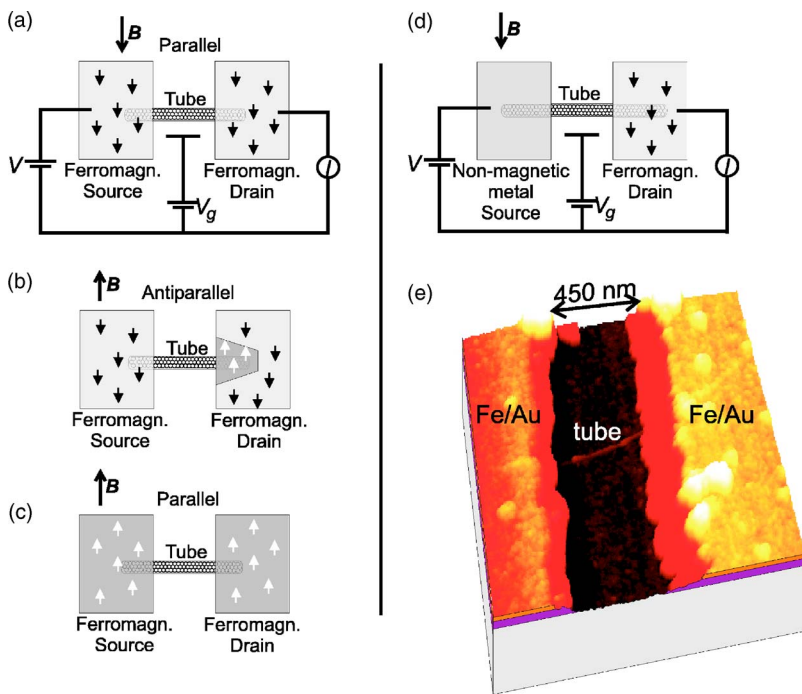


FIG. 1. Schematics of our devices and the measurement setup. The bias voltage V is applied to the source, and I is measured from drain to ground. V_g is applied to the capacitively coupled back gate. (a)–(c) A SWNT contacted by two ferromagnetic terminals (Fe-NT-Fe and FS-NT-FS). When the field is swept, the tube may be contacted by alternating parallel and antiparallel magnetized domains. (d) A SWNT contacted by a nonmagnetic metal source and a ferromagnetic semiconductor drain (M-NT-FS). (e) (Color on-line) Atomic force microscopy of the device Fe-NT-Fe2.

quantum dot devices. From Fig. 2(a) it emerges that the magnetic field has a significant gate independent influence on the conductance. The Coulomb blockade oscillations are present for all B fields. At $B = -0.05$ T, where G is suppressed, the amplitude of the oscillations is suppressed too. The influence of B is measured directly in the magnetic field sweep Fig. 2(b), which reveals a hysteretic dip in the conductance, i.e., a significant magnetoresistance (MR), shortly after passing $B = 0$ T. The MR evolves with decreasing temperature, and at the lowest temperature the conductance is almost completely quenched. All traces in B are averages over several individual traces, in order to validate the consistency in our measurements. Figures 2(c) and 2(d) are examples of B sweeps measured at 4.2 and 9 K for a similar device. These measurements show a similar form of hysteretic MR, though the hysteretic features show up with opposite signs, i.e., both positive and negative MR can be observed.

We now turn to the (Ga,Mn)As contacted tubes. The Curie temperature of the (Ga,Mn)As is in the order of 70 K as determined from transport measurements.¹⁷ Consequently the lead material is magnetic at the temperatures relevant for this study. The in-plane coercive field of the (Ga,Mn)As terminals is determined from MR measurements on the (Ga,Mn)As material, where the switching of the magnetization is found as a maximum in resistance at about 0.05 T. The magnetoresistance of the (Ga,Mn)As is a few ohms, which is negligible compared to the low temperature resistance of the tube devices of several megaohms. Periodic Coulomb blockade oscillations and single-quantum-dot formation in the tube devices with ferromagnetic semiconductor terminals are presented elsewhere,¹⁷ and the data clearly resemble what is seen in tube devices with normal metal terminals.

Figure 3(a) illustrates measurements of hysteretic MR for FS-NT-FS at $T = 14$ K, 2 K, and 310 mK. At the lowest temperature, a finite source-drain voltage is applied in order to

overcome the vanishing conductance in the linear regime. The magnitude of the hysteretic behavior increases with decreasing temperature. Measurements at $T = 310$ mK are presented in Fig. 3(b) for source-drain voltages of 4 and 2 mV, respectively. The first has a dip structure, while the second shows a more pronounced peak structure. This particular sign alternation of the hysteretic MR as a function of source-drain voltage is found reproducible in a small V_g range in one cool down. Otherwise, the MR behavior often shifts irregularly, under various source-drain and gate voltage conditions and during different cooling cycles. The graphs shown here have been chosen to illustrate the diversity in our measurements.

In Fig. 4 we present data on a reference device with one normal and one ferromagnetic terminal (M-NT-FS). G vs B at 4.2 K is presented in Fig. 4(a) for two different V_g . Hysteretic MR behaviors are recorded in this device type too, and peak as well as dip behaviors are observed. Examples of this are presented in Fig. 4(a). The alternations between hysteretic dips or peaks are not related to the gate or source-drain voltage in a simple manner.

In this paper we have presented measurements on different types of ferromagnetically contacted SWNT devices. In devices with two ferromagnetic terminals, i.e., Fe-NT-Fe and FS-NT-FS structures, hysteretic MR features have been observed to reach zero conductance at 350 mK. The hysteretic features always appear in the vicinity of zero magnetic field, with the dominant feature emerging after the sweeping field passes through zero. At higher values of the applied magnetic field ($|B| \gtrsim 0.2$ T), the conductance does not display any hysteresis, as G is symmetric in B and independent of the sweep directions. The hysteretic MR feature appears as either a dip or a peak in the conductance. Some devices display solely dip or peak structures, whereas others fluctuate in a noncontrollable manner between peak and dip behavior. In order to quantify the hysteretic MR we define the magni-

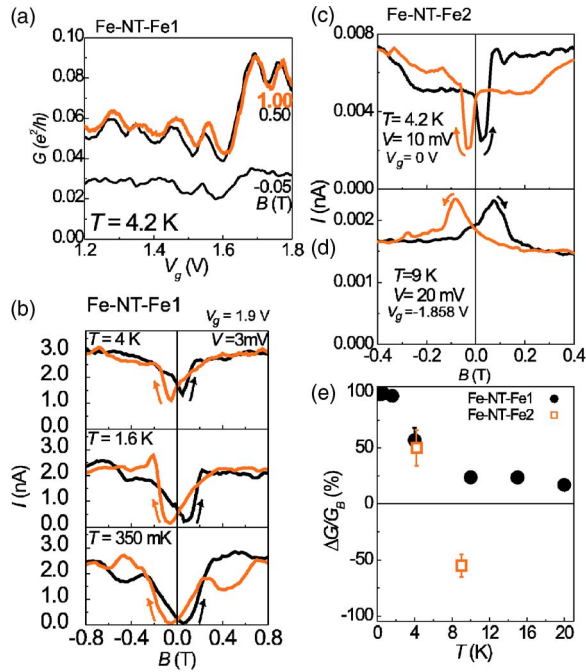


FIG. 2. (Color online) Fe-NT-Fe devices. (a) Fe-NT-Fe1. G vs V_g at $T=4.2$ K for $B=1$ (bold), 0.5 , and -0.05 T. (b) Fe-NT-Fe1. I vs B measured at $T=4$ K, 1.6 K, and 350 mK. Sweep-up and sweep-down directions are indicated by the arrows. All curves of I vs B are the average of 5–10 individual traces. (c) Fe-NT-Fe2 [see Fig. 1(c)]. I vs B with applied source-drain voltage $V=10$ mV at $T=4.2$ K. (d) Fe-NT-Fe2. The second cool down at $T=9$ K. I vs B at $V=20$ mV, averaged over 20 traces. (e) The averaged magnitude of the MR plotted for the two devices Fe-NT-Fe 1 and 2 vs T . The points and error bars display the mean value and the variance of the MR measured for the devices Fe-NT-Fe 1 and 2.

tude of the hysteretic MR as $\Delta G/G_B = (G_B - G_{ex})/G_B$ where G_{ex} is the conductance at the hysteretic extremum (dip or peak), and G_B is the conductance at the same magnetic field, but measured during the reverse sweep. In the nonlinear regime, we define similarly $\Delta G/G_B = (I_B - I_{ex})/I_B$. Figures 2(e), 3(c), and 4(b) sum up the mean values of the hysteretic behaviors found in our devices. The diversity in the hysteretic MR when varying V_g and V and cycling the temperature is presented by error bars, which show the variance from all our measurements on a given device. We have observed hysteretic features of magnitudes up to almost 100% and down to -150% , with a rapid increase at the lowest temperatures, which is visible in spite of the large diversity found in our measurements. Hysteretic MR features are observed in devices with one ferromagnetic terminal, too. These features are not as clearly defined as in devices with two ferromagnetic terminals, but the relative amplitude is large (roughly 10%). The temperature dependence of the amplitude is less dramatic than that for devices with two ferromagnetic terminals. Hysteretic MR has not been observed in devices with exclusively nonmagnetic terminals, e.g., Cr/Au.

More than 30 conducting Fe-NT-Fe devices have been examined, yet only four of these display any hysteretic MR. In contrast, all investigated devices with terminals of (Ga,Mn)As, 15 FS-NT-FS and three M-NT-FS, inevitably

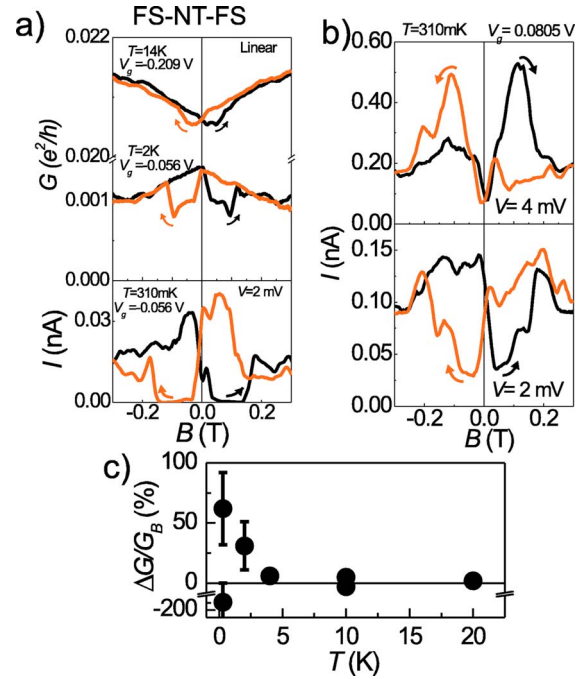


FIG. 3. (Color online). FS-NT-FS device. (a) G or I vs B , measured at $T=14$ K, 2 K, and 310 mK. (b) I vs B at $T=310$ mK with applied source-drain voltages of $V=4$ and 2 mV. All B curves are averaged over about eight individual measurements. (c) The hysteretic behavior vs T . The points and error bars display the mean value and the variance of the MR measured for the device FS-NT-FS.

show MR. We speculate that the absence of MR in many of the Fe-NT-Fe devices could be related to the architecture of these devices. It is possible that the Au cap layer bypasses the Fe contact material, so the tubes are not contacted by ferromagnetic material, but rather are of the form Au-NT-Au. Moreover, oxidation of the Fe terminals may critically destroy the ferromagnetic properties of the contacts.

SWNTs have no intrinsic magnetoresistance at fields relevant for the present measurements, and magnetoresistance in the terminals alone cannot account for the large magnitude of the observed hysteretic behavior. The hysteretic dips or peaks occur preferentially after the field has been swept through zero, and in the range of the coercive field. This shows that the hysteresis must be related to the occurrence and switching of magnetic domains, which couple to the tubes. Most often, the changes in the conductance are abrupt, indicating that only one or a few domains in each terminal are actively involved in the coupling to the tubes. During each measurement, G vs B follows the same track repeatedly, indicating a reproducible change of domain configuration vs B . The hysteretic MR may be interpreted as sign of spin-polarized transport through the nanotube. However, we find the prevailing theoretical models incomplete. To our knowledge, no existing model is capable of explaining our observations of the almost 100% ratio of the MR, the change of sign in the effect, as well as the presence of MR in devices with a single ferromagnetic terminal.

It is found that the absolute magnitude of the positive or negative hysteretic behavior increases with decreasing temperature. A surprising increase of the hysteretic MR of up to

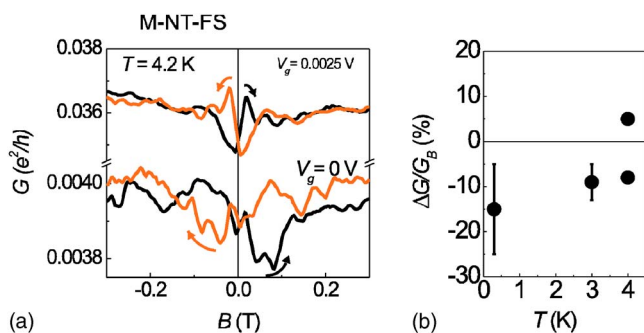


FIG. 4. (Color online). M-NT-FS device. (a) $T=4.2$ K. G vs B with $V_g=0$ and 0.0025 V (average over ten individual measurements). (b) The mean value and the variance of the magnitude of the hysteresis vs T for the device M-NT-FS.

100% occurs in the low temperature limit [see Figs. 2(e) and 3(c)] where the conductance is highly suppressed due to strong Coulomb blockade in the device. This temperature regime is far below the Curie temperature of terminal materials; therefore the polarization of the current-carrying electrons in the terminals may not account for such dramatic temperature dependence. Likewise, it is unlikely that this dramatic temperature dependence of the hysteretic behavior can be justified from temperature dependence in the spin-relaxation length. A source of magnetoresistance in ferromagnet–quantum dot–ferromagnet structures has been demonstrated by Shimada *et al.*,⁵ where the change in spin-up chemical potential in the electrode in a strong magnetic field competes with the Coulomb blockade energy. This could lead to a shift in the gate dependence of the Coulomb blockade oscillations in our samples, were it not for the fact that our Coulomb blockade energy is at least an order of magnitude larger and the magnetic field applied an order of

magnitude smaller than in the experiments by Shimada *et al.*⁵ We therefore do not observe this magnetoresistance contribution.

We believe it is important to gain a better understanding of the electrical contact between the ferromagnetic terminals and the nanotubes in order to explain our observed MR effects in ferromagnetically contacted SWNTs. Scanning probe experiments by Céspedes *et al.*²⁰ reveal evidence of contact-induced magnetism in multiwall carbon nanotubes placed on a ferromagnetic substrate. This work indicates an interesting route for exploring electrical and magnetic coupling between ferromagnets and nanotubes. Experiments by Gould *et al.*²¹ on tunnel magnetoresistance from a single layer of (Ga,Mn)As display a spin-valve effect, referred to as tunneling anisotropic magnetoresistance. The magnitude of the MR measured in our M-NT-FS devices at 4 K is comparable to the results by Gould *et al.*

In conclusion, we have presented experimental results on two-terminal SWNT devices with one and two ferromagnetic terminals. These devices show a large diversity of sign and magnitude of the hysteretic MR. Yet, an overall increase in magnitude of the effect is found when decreasing the temperature, and we see a complete quenching of G at $T=350$ mK. Our observations call for detailed understanding of spin-polarized transport between the tube and the contacting terminals.

We acknowledge fruitful discussions with Pavel Štěřda, Jørn Borggreen, and Bruce Alphenaar, and thank Jørn Bindlev Hansen for a critical reading of the manuscript, and Janusz Sadowski for MBE growth at III-V Nanolab (NBIfAPG, University of Copenhagen and Research Center Com, Technical University of Denmark) and at MAX-lab (Lund University). NEDO Spintronics and the Danish Research Councils (STVF and SNF) supported this work.

*Electronic address: ane@fys.ku.dk

- ¹I. Žutić, J. Fabian, and S. D. Sarma, *Rev. Mod. Phys.* **76**, 323 (2004).
- ²M. Zaffalon and B. J. van Wees, *Phys. Rev. Lett.* **91**, 186601 (2003).
- ³C.-M. Hu, J. Nitta, A. Jensen, J. B. Hansen, and H. Takayanagi, *Phys. Rev. B* **63**, 125333 (2001).
- ⁴K. Tsukagoshi and B. W. Alphenaar, *Nature (London)* **401**, 572 (1999).
- ⁵H. Shimada, K. Ono, and Y. Ootuka, *J. Phys. Soc. Jpn.* **67**, 1359 (1998).
- ⁶*Carbon Nanotubes: Synthesis, Structure, Properties, and Applications*, edited by M. S. Dresselhaus, G. Dresselhaus, and Ph. Avouris, *Topics in Applied Physics* vol. 80 (Springer-Verlag, Berlin, 2001).
- ⁷P. L. McEuen, M. Fuhrer, and H. Park, *IEEE Trans. Nanotechnol.* **1**, 78 (2002).
- ⁸J. Nygård, D. H. Cobden, M. Bockrath, P. L. McEuen, and P. E. Lindelof, *Appl. Phys. A: Mater. Sci. Process.* **69**, 297 (1999).
- ⁹M. Julliere, *Phys. Lett.* **54A**, 225 (1975).

- ¹⁰S. Sahoo, T. Kontos, C. Schönenberger, and C. Sürgers (unpublished).
- ¹¹D. Orgassa, G. J. Mankey, and H. Fujiwara, *Nanotechnology* **12**, 281 (2001).
- ¹²X. Hoffer, C. Klinke, J.-M. Bonard, L. Gravier, and J.-E. Wegrowe, *Europhys. Lett.* **67** (2004).
- ¹³B. Zhao, I. Mönch, T. Mühl, H. Vinzelberg, and C. M. Schneider, *J. Appl. Phys.* **91**, 7026 (2002); B. Zhao, I. Mönch, H. Vinzelberg, T. Mühl, and C. M. Schneider, *Appl. Phys. Lett.* **80**, 3144 (2002).
- ¹⁴J.-R. Kim, H. M. So, J.-J. Kim, and J. Kim, *Phys. Rev. B* **66**, 233401 (2002).
- ¹⁵A. Jensen, J. Nygård, and J. Borggreen, in *Proceedings of the International Symposium on Mesoscopic Superconductivity and Spintronics*, edited by H. Takayanagi and J. Nitta (World Scientific, Singapore, 2003), p. 33.
- ¹⁶P. R. Poulsen, J. Borggreen, J. Nygård, D. H. Cobden, M. M. Andersen, and P. E. Lindelof, in *Electronic Properties of Novel Materials—Molecular Nanostructures*, edited by H. Kuzmany, J. Fink, M. Mehring, and S. Roth, *AIP Conf. Proc. No 544* (AIP, Melville, NY, 2000), p. 504.

- ¹⁷A. Jensen, J. R. Hauptmann, J. Nygård, J. Sadowski, and P. E. Lindelof, *Nano Lett.* **4**, 349 (2004).
- ¹⁸S. J. Tans, M. H. Devoret, H. Dai, A. Thess, R. E. Smalley, L. J. Geerligs, and C. Dekker, *Nature (London)* **386**, 474 (1997).
- ¹⁹M. Bockrath, D. H. Cobden, J. Lu, A. G. Rinzler, R. E. Smalley, L. Balents, and P. L. McEuen, *Nature (London)* **397**, 598 (1999).
- ²⁰O. Céspedes, M. S. Ferreira, S. Sanvito, M. Kociak, and J. M. D. Coey, *J. Phys.: Condens. Matter* **16**, L155 (2004).
- ²¹C. Gould, C. Rüster, T. Jungwirth, E. Girgis, G. M. Schott, R. Giraud, K. Brunner, G. Schmidt, and L. W. Molenkamp, *Phys. Rev. Lett.* **93**, 117203 (2004).